Available online at www.sciencedirect.com
SCIENCE DIRECT®
Synthetic Metals 153 (2005) 81–84
SYNTHETIC METALS
www.elsevier.com/locate/synmet

Novel Regiospecific MDMO-PPV Polymers with Improved Charge Transport Properties for Bulk Heterojunction Solar Cells

A. J. Mozer[a]*, P. Denk[a], M. C. Scharber[a], H. Neugebauer[a], N. S. Sariciftci[a], P. Wagner[b,†], L. Lutsen[b], D. Vanderzande[b] A. Kadashchuk[c], R. Staneva[d], R. Resel[d]

[a]*Linz Institute for Organic Solar Cells (LIOS), Johannes Kepler University Linz, Altenbergerstrasse 69, A-4040 Linz, Austria*
[b]*IMEC, IMOMEC division, Organic and Polymer Chemistry Group, Wetenschapspark 1, Diepenbeek, B-3590, Belgium*
[c]*Institute of Physics, National Academy of Sciences of Ukraine, Prospect Nauky 46, 03028 Kyiv, Ukraine*
[d]*Institute of Solid State Physics, Graz University of Technology, Petersgasse 16, A-8010 Graz, Austria*

Abstract

A series of novel regiospecific MDMO-PPV polymers have been synthesized by the copolymerization of the mixture of the two isomers of the asymmetrically substituted monomer via the sulphinyl precursor route. As the weight percent of either one of the two isomers is increased above ~ 80 percent, the solubility of the resulting polymer is reduced. This is attributed to enhanced interchain ordering in the solid as evidenced by X-ray diffraction measurements. The hole mobility of the polymer prepared by the copolymerization of the 70:30 weight percent mixture of the two isomers (70:30 RS-MDMO-PPV) is found to be a factor of ~3.5 higher at all measured electric fields at room temperature as compared to the regiorandom MDMO-PPV (RRa-MDMO-PPV). The electric field and temperature dependence of the hole mobility is discussed in the framework of disorder formalism and reveals an interplay between the one order of magnitude higher prefactor mobility and the slightly increased energetic disorder. Such behavior is attributed to the presence of ordered regions embedded in an otherwise amorphous matrix. The mobility is expected to increase within the ordered regions due to better electronic coupling. On the other hand, such regions may act as traps for the charge carriers, as it is supported by thermally stimulated luminescence measurements. Finally, bulk heterojunction photovoltaic devices based on the blends of 70:30 MDMO-PPV and the methanofullerene PCBM with improved power conversion efficiency and a high (0.71) filling factor have been fabricated.

Keywords: Photoconductivity, transport measurements, poly(phenylene vinylene) derivatives, fullerenes and derivatives, solar cells

1. Introduction

The effect of charge carrier mobility on the performance of bulk heterojunction solar cells based on the blend of the conjugated polymer MDMO-PPV and the soluble fullerene derivative PCBM is a focus of current scientific interest [1]. It has been reported that the hole mobility in MDMO-PPV films is 2 to 4 orders of magnitude lower than the electron mobility in PCBM films. This indicates that to improve the performance of the photovoltaic devices, the hole mobility of MDMO-PPV needs to be increased [2]. In search for a polymer with higher charge carrier mobility, we have synthesized a series of novel regiospecific MDMO-PPV polymers using the sulphinyl precoursor synthetic route [3]. For detailed charge transport studies, we have chosen the well soluble polymer based on the 70:30 weight percent mixture of the monomers. The temperature and electric field dependence of the mobility has been determined by a time-of-flight technique, and the data is analyzed in the framework of disorder formalism [4]. The improved properties of the regiospecific MDMO-PPV copolymer has been utilized in fabrication of efficient photovoltaic devices with high filling factor.

2. Experimental

2.1. Materials and Sample Preparation

The synthesis of the regiospecific MDMO-PPV polymers is described in detail in [5]. Regiorandom MDMO-PPV was purchased from Covion GmbH. Thin film samples for the photoluminescence (PL), thermally stimulated luminescence (TSL) and time-of-flight mobility (ToF) have been prepared by the doctor blade technique from chlorobenzene solution onto microscope slides (PL, TSL) or structured ITO-coated glass substrates (ToF). On

* Corresponding author: attila.mozer@jku.at
† Present address: Nanomaterials Research Centre, Massey University, Private Bag 11 222 Palmerston North, New Zealand

0379-6779/$ – see front matter
doi:10.1016/j.synthmet.2005.07.151

top, Al was evaporated as cathode in vacuum better than 10^{-5} mbar.

2.2. UV-vis Absorption, Photoluminescence(PL) and X-ray Diffraction (XRD)

The thin film samples for the PL measurements were mounted into a cryostat and illuminated from the front side by the 514 nm line of an Ar^+ laser (0.3 mW). A lowpass filter was used to block the Ar^+ excitation line, and the collected light was dispersed by a L=1/8 m monochromator and detected by a Si photodetector array. XRD measurements were performed on a Siemens D 501 diffractometer in θ–2θ *Bragg-Brentano* geometry using CuK_α radiation selected with a monochromator. The voltage and current were set at 40 kV and 30 mA. The sample powder was investigated on a low reflectance silicon single crystal substrate.

2.3. Time-of-Flight Mobility Setup

The samples were mounted in a liquid nitrogen cooled cryostat, and illuminated by 3 ns, 532 nm pulses of a Nd:YAG pulsed laser. The photocurrent transients were amplified by a low noise current amplifier and recorded by a digitizing oscilloscope. The transit time (t_{tr}) of the charge carriers is defined as the meeting point of the asymptotes of the two linear regimes in the log photocurrent vs. log time plots. The ToF mobility (μ) was calculated as $\mu=d^2/(V\times t_{tr})$ in $cm^2V^{-1}s^{-1}$ units, where d is the film thickness, V is the applied potential.

2.4. Thermally Stimulated Luminescence (TSL)

Thermally stimulated luminescence (TSL) measurements were carried out using a home-built system operable from 4.2 to 350 K using a temperature controlled helium cryostat. After cooling down to 4.2 K, the samples were photoexcited (typically for 30 sec) using different emission lines of a high-pressure 500 W mercury lamp separated by a set of appropriate glass filters. After the photoexcitation, the TSL was detected in a photon-counting mode with a cooled photomultiplier, positioned immediately next to the cryostat window. The measurements were performed at the constant heating rate $\beta = 0.15$ K/s.

2.5. Photovoltaic Device Preparation and Characterization

The photovoltaic devices based on the 1:4 w% mixture of 70:30 RS-MDMO-PPV polymer and PCBM were prepared and the devices were characterized as it is described in ref. [5]. The power conversion efficiency of the solar cells under simulated AM 1.5 conditions was calculated as:

$$\eta_{AM1.5}[\%]=\left(\frac{P_{out}\times m}{P_{in}}\right)\times 100=\frac{FF\times V_{oc}\times J_{sc}\times m}{P_{in}}\times 100 \qquad (1)$$

where P_{out} [mW cm^{-2}] is the output electrical power of the device, P_{in} [mW cm^{-2}] is the light intensity incident on the sample, and m is the spectral mismatch factor, FF is the filling factor defined as $FF=(V_{mpp}\times J_{mpp})/(V_{oc}\times J_{sc})$, where V_{mpp} [V], and J_{mpp} [mA cm^{-2}] are the maximum voltage and maximum current density at the maximum power point, respectively, V_{oc} [V] is the open-circuit voltage, J_{sc} [mA cm^{-2}] is the short-circuit current density. The incoming light intensity was 80 mW cm^{-2}, and the spectral mismatch factor was 0.753. A simulation of the current density vs. voltage curves were performed based on a simple one-diode equivalent circuit model in the following form:

$$J=J_0\left(\exp\left(\frac{V-JR_{RS}}{nk_BT}\right)-1\right)+\frac{V-JR_{RS}}{R_P}-J_{SC} \qquad (2)$$

where J [A cm^{-2}] and V [V] are the measured current density and voltage values, respectively, J_0 [A cm^{-2}] is the reverse bias dark current, R_s [Ω cm^{-2}] is the series resistance, R_p [Ω cm^{-2}] is the parallel resistance and J_{sc} [A cm^{-2}] is the short-circuit current density under illumination.

3. Results

3.1 General Properties

Fig. 1. shows the θ –2θ-scans of selected MDMO-PPV polymers measured by XRD powder diffraction. The numbers in the bracket indicates the ratio (weight percent) of the two isomers of the asymmetrically substituted monomer in reaction mixture, for e.g. 0:100 MDMO-PPV stands for the 100 percent homopolymer, meanwhile 50:50 MDMO-PPV means the 50:50 mixture of the two isomers. As the regioregularity increases, a clearly distinguished reflection peak develops at around 3 degrees, corresponding to an intermolecular distance of 28.5 Å. The exact position of this peak was determined by small angle X-ray scattering measurement. It corresponds to the repeating distance between the polymer backbones separated by side chains. The broad maximum at ~20 degrees is assigned to the amorphous halo of the polymer.

Correspondingly, the solubility of the MDMO-PPV copolymers is greatly reduced as the ratio of either one of the two isomers of the monomer is increased above 80%, which makes them unusable for further characterization techniques based on solution-based sample preparation. Therefore, we have chosen the well soluble polymer 70:30 RS-MDMO-PPV for further investigation, and compare its optical, charge transport and photovoltaic properties in bulk heterojunction solar cells with that of the commercially available regiorandom MDMO-PPV.

3.2. Absorption and Photoluminescence

The absorption maximum of the 70:30 RS-MDMO-PPV copolymer measured in dilute chlorobenzene solution (not shown) is ~10 nm red shifted as compared to its regiorandom counterpart, which is indicative of longer

effective conjugation length, and more stretched conformation of the conjugated chains. The bands in the PL spectra of the films prepared from the lower concentration (0.25 w%) chlorobenzene solutions are ~ 40 nm red shifted (Fig. 2. curve 1) as compared to the solution spectra, and the lower energy features found between at 620 nm – 700 nm are selectively enhanced and further red shifted. The PL bands of the 70:30 RS-MDMO-PPV films are slightly red shifted as compared to the RRa-MDMO-PPV indicating that the more stretched conformation is maintained in these films. The above mentioned features around 620 nm – 700 nm are even more enhanced in the films prepared from 1 w% solutions, which is highly indicative of the formation of interchain species in the films of these conjugated polymers [7].

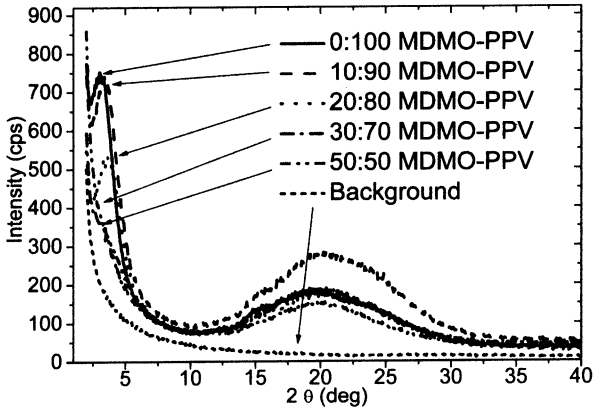

Fig. 1: θ / 2θ-scans of the MDMO-PPV polymer powders.

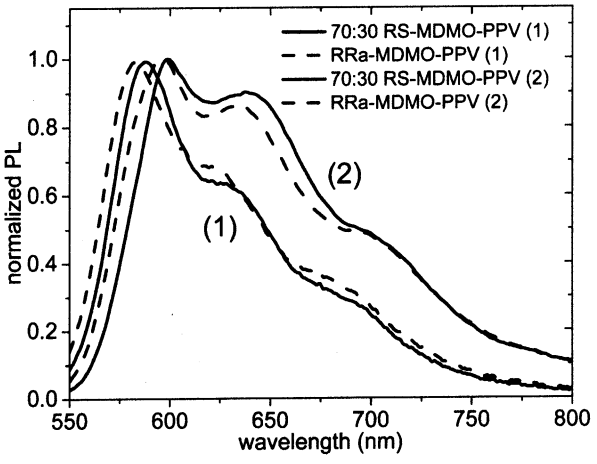

Fig. 2: Normalized photoluminescence spectra measured in films prepared from (1) 0.25 w% (2) 1 w% chlorobenzene solution of the 70:30 RS-MDMO-PPV and RRa-MDMO-PPV polymers.

3.3. Time-of-Flight Mobility

The room temperature ToF mobility of the 70:30 RS-MDMO-PPV polymer is compared to that of RRa-MDMO-PPV in Fig. 3. The ToF mobility of the former is ~3.5 times higher at all measured electric fields. Interestingly, we did not observe a significant change in the measured mobility values by changing the film thickness, which shows that the film morphology is not altered as far as the charge carrier mobility at room temperature is concerned.

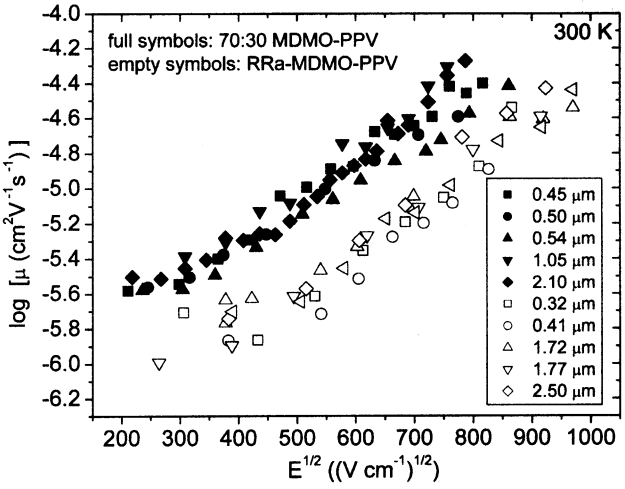

Fig. 3: Room temperature electric field dependent ToF mobility of the MDMO-PPV polymers measured at various film thicknesses.

Previous studies showed that decreasing the on-chain chemical defects can increase the mobility significantly by reducing the concentration of charge carrier traps [8]. On the other hand, increasing the regioregularity may decrease the energetic disorder [9]. In order to distinguish which mechanism may be responsible in our samples, we have measured the temperature and electric field dependence of mobility, and analyzed the data in the framework of disorder formalism (eq. 3) [4].

$$\mu = \mu_0 \exp\left[-\frac{2}{3}\left(\frac{\sigma}{kT}\right)^2\right] \exp\left[C\left(\left(\frac{\sigma}{kT}\right)^2 - \Sigma^2\right)E^{1/2}\right] \quad (3)$$

where σ [eV] is the width of the Gaussian density of states, Σ is a parameter characterizing positional disorder, μ_0 [$cm^2V^{-1}s^{-1}$] is a prefactor mobility, and C is a fit parameter.

The calculated values of μ_0, σ and C together with room temperature mobility values (μ_{RT}) measured at 5×10^5 Vcm^{-1} electric field are summarized in Table 1. The prefactor mobility, which is related to the electronic coupling between the charge transport sites, is one order of magnitude higher of the 70:30 RS-MDMO-PPV, and the σ is also increases slightly. This result is proposed to originate from the better charge transport within the ordered regions embedded in an otherwise amorphous matrix. The mobility in the ordered regions is expected to be higher due to better electronic overlap between the adjacent sites. The energy of the charge carriers within these ordered regions, on the other hand, maybe lower due to the increased dipole - induced dipole interaction between the charge carriers and the more extended π-conjugated electronic systems, acting as charge carrier traps at lower temperatures.

TABLE 1. Room temperature mobility (μ_{RT}), prefactor mobility (μ_0), energetic disorder (σ) and C (see Eq. 3).

Sample[1]	μ_{RT} [$cm^2 V^{-1}s^{-1}$]	μ_0 [$cm^2V^{-1}s^{-1}$]	σ [meV]	C [$(cmV^{-2})^{1/2}$]
1	2.8×10^{-5}	2.6×10^{-3}	115	1.54×10^{-4}
2	0.85×10^{-5}	0.22×10^{-3}	105	1.35×10^{-4}

[1]Sample 1 and 2 stands for 70:30 RS-MDMO-PPV and RRa-MDMO-PPV, respectively.

3.3. Thermally Stimulated Luminescence (TSL)

Fig. 4. shows the measured TSL curves of the RRa-MDMO-PPV and the 70:30 RS-MDMO-PPV polymers. The TSL curves were deconvoluted into two Gaussian distributions shown by solid lines. In the case of the 70:30 RS-MDMO-PPV polymer, the high temperature band at ~100 K is relatively increased with respect to the 50 K band. The higher temperature peak in this class of polymers has been previously assigned to recombination of charge carriers thermally liberated from lower lying structural traps[10]. The selectively increased higher energy TSL peak measured for the 70:30 MDMO-PPV copolymer suggests the presence of higher concentration of these traps in accordance with the finding of the temperature dependence charge transport studies.

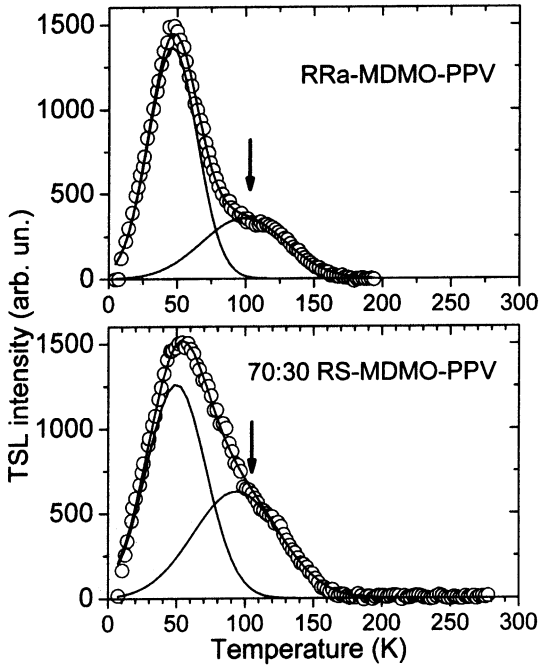

Fig. 4: Thermally Stimulated Luminescence (TSL) curves recorded for RRa-MDMO-PPV (upper) and 70:30 RS-MDMO-PPV (lower). The solid lines represent fits of Gaussian line shapes to the experimentally measured curves.

3.4. Photovoltaic Devices

The improved charge transport property of the 70:30 RS-MDMO-PPV polymer have been utilized in fabrication of bulk heterojunction solar cells. The photovoltaic device properties and the diode parameters calculated using a simple one diode model are compared in Table 2. Although the short circuit current density and the open circuit voltage are quite similar, the power conversion efficiency (η) of the photovoltaic devices based on the 70:30 RS-MDMO-PPV is increased due to the higher filling factor (FF). The simulation according to eq. 2 reveals that the higher parallel resistance together with the smaller series resistance is responsible for the high filling factor. The former is thought to be related to for e.g. improved film property; however the latter may be indicative of the increased charge carrier mobility in the photoactive blends as suggested by the ToF studies of the pristine MDMO-PPV polymers.

TABLE 2. Photovoltaic performance of the bulk heterojunction solar cells, and the parameters of eq. 2. (The units are defined in Section 2.5.)

	J_{sc}	V_{oc}	FF	η	J_0	R_s	R_p	n
1	5.0	0.8	0.71	2.65	6×10^{-7}	1.3	2150	1.9
2	5.25	0.82	0.61	2.5	6×10^{-7}	3	950	2.0

Sample 1 and 2 stands for 70:30 RS-MDMO-PPV and RRa-MDMO-PPV, respectively.

4. Conclusions

A series of novel regiospecific MDMO-PPV polymers has been synthesized via the sulphinyl precursor route. The charge transport properties of the 70:30 RS-MDMO-PPV has been studied by a ToF technique. A comparison of the temperature and electric field dependence of the mobility of this regiospecific copolymer with its regiorandom counterpart reveals the interplay between the molecular structure – film morphology – charge transport properties. The improved properties of the novel MDMO-PPV copolymer are also demonstrated in fabrication of bulk heterojunction solar cells with very high filling factors.

Acknowledgments

The financial support of the European Commission within the framework of the Human Potential-Research Training Network, EUROMAP"contract no. HPRN-CT-2000-00127.

References

[1] S. A. Choulis, J. Nelson, Y. Kim, D. Poplavskyy, T. Kreouzis, J. R. Durrant, D. D. C. Bradley, Appl. Phys. Lett. 83 (2003) 3812 – 3814.
[2] V.D. Mihailetchi, et al., Adv. Mater. 13 (2003) 43.
[3] L. Lutsen, P. Adriaensens; H. Becker, A. J. van Bremen, D. Vanderzande, J. Gelan, Macromolecules 32 (1999) 6517.
[4] H. Bässler, Phys. Status Solidi b 175 (1993) 15.
[5] A. J. Mozer, P. Denk, M. C. Scharber, H. Neugebauer, N. S. Sariciftci, P. Wagner, L. Lutsen, D. Vanderzande, J. Phys. Chem. B 108 (2004) 5235.
[6] M. Ballauff, G. F. Schmidt, Macromol. Chem., Rapid Commun. 8 (1987) 93.
[7] T.-Q. Nguyen, V. Doan, J. B. Schwartz, J. Chem. Phys. 110 (1999) 4068.
[8] J. Veres et al.. In IS&T's NIP16: International Conference on Digital Printing Technologies; IS&T.: Vancouver, 2000; pp 335.
[9] Martens et al. Phys. Rev B 61 (2000) 7489.
[10] A. Kadashchuk, et al. *J. Appl. Phys.* 91 (2002) 5016.